

Ballistic SNS sandwich as a Josephson junction

Edouard B. Sonin*

Racah Institute of Physics, Hebrew University of Jerusalem, Givat Ram, Jerusalem 9190401, Israel

(Dated: September 9, 2021)

The paper develops the theory of the ballistic SNS sandwich, in which the Josephson effect exists without the proximity effect. The theory takes into account restrictions imposed by the charge conservation law and the incommensurability of the superconducting gap with the Andreev level energy spacing. This resulted in revisions of some conclusions of previous works. In the one-dimensional case the Josephson phase of the ground state of the ballistic SNS sandwich is not necessarily zero but may have any value from 0 to π . If this value is π this is a π junction, which was well known before. The suppression of the supercurrent at temperatures on the order or higher than the Andreev level energy spacing, which was predicted in previous investigations, does not take place in the one-dimensional case.

At zero temperature the ballistic SNS sandwich of any dimensionality is not a weak link. This leads to unusual properties: the absence of the Josephson plasma mode localized at the normal layer and the Meisner effect with the same London penetration depth in the normal and the superconducting layers.

I. INTRODUCTION

Originally the Josephson junction was considered as an insulator or normal metal bridge between two superconductors. The Josephson coupling between superconductors was provided due to penetration of the superconducting order parameter into the bridge (proximity effect) if the bridge is not too long compared with the coherence length. However, it was noticed long ago [1–3] that if the bridge is a ballistic normal metal the Josephson coupling is possible even for rather long bridges. This was demonstrated in an idealized model of the ballistic SNS sandwich (planar SNS Josephson junction). There is a normal layer of width L between two superconductors. The layers are perpendicular to the axis x (Fig. 1). The effective masses and Fermi energies are the same in the superconductors and in the normal metal. The only difference is that the pair potential sharply vanishes in the normal layer $-L/2 < x < L/2$. Investigations of this model continue up to now [4]. The ballistic SNS Josephson junction was studied for unconventional pairing in high- T_c superconductors [5]. There were theoretical and experimental investigations for other materials bridging two superconductors: graphene [6, 7], topological insulator [8], and nanotubes [9].

Previous theoretical investigations of the ballistic SNS sandwich have left some questions unanswered up to now. Ishii [2] noticed that canonical relations for the pair of Hamiltonian conjugated variables “charge–phase” were not satisfied. There was a problem with the charge conservation law because the theory postulated some spatial distribution of the order parameter (gap) without solving the self-consistency equation for gap, which determines this distribution. There were also disagreements on the final form of the current–phase relation.

The present paper suggests an approach free of those flaws. In particular, restrictions imposed by the charge conservation law were checked. This resulted in a revision of some previous results. The charge conservation law can be satisfied only taking into account three contributions to the total current: (i) The current induced by the phase gradient in the superconducting layers. We shall call it the Cooper-pair condensate, or simply condensate current. (ii) The current, which can flow in Andreev states even if the Cooper-pair condensate is at rest and all Andreev states are empty. It will be called vacuum current. (iii) The current induced by nonzero occupation

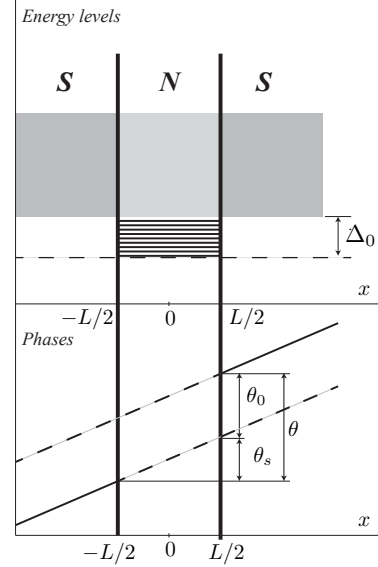


FIG. 1. Energy levels and phases in the SNS sandwich. The interval of continuum states is shaded. The Andreev bound states inside the gap Δ_0 are shown by solid lines. The lower part of the figure shows the bound-state phase θ_0 , the superfluid phase θ_s , and the Josephson phase θ .

* sonin@cc.huji.ac.il

of Andreev states, i.e., by creation of quasiparticles. It will be called excitation current. The condensate motion produces the same current in superconducting and normal layers of the SNS sandwich, while vacuum and excitation currents, which are connected with the Andreev states, exists only in the normal layer. The charge conservation law requires that in a stationary state the total current in all layers must be the same. Thus, the sum of the vacuum and the excitation currents must always vanish.

Our analysis revealed the effect of incommensurability of the spectrum gap in the superconducting layers to the Andreev level energy spacing in one-dimensional (1D) case, when normal and superconducting layers become normal and superconducting segments of a 1D wire. The effect is important up to high temperatures. Here and later on low or high temperatures mean temperatures much lower or much higher than the Andreev level energy spacing, but still always much lower than the superconducting gap. Due to the incommensurability effect, in the ground state of the SNS sandwich the phase difference θ across the SNS sandwich is not necessarily zero, but may vary from zero to π . In the past Josephson junctions with the ground state at the phase difference $\pm\pi$ were well known and called π junctions. In analogy with this, we shall call junctions with the phase difference θ in the ground state θ junctions. Josephson π junctions were predicted and observed in ferromagnetic junctions [10], junctions with unconventional superconductivity [11], quantum dot junctions [12], and SINIS junctions [13]. The transition from 0 to π junction was observed in carbon nanotube Josephson junctions [9] (see further discussion in the concluding section IX). Another outcome of our analysis is that strong suppression of the supercurrent at temperatures comparable or higher than the Andreev level energy spacing, which was predicted in previous investigations [1–3], does not take place in 1D systems.

Sometimes at currents smaller than critical values not only the sum of the vacuum and excitation currents vanish, but any of them vanishes separately. This takes place in 1D systems at any temperature and in systems of any dimensionality at zero temperature. Thus, the charge is transported only by the moving condensate, and the phase distribution does not differ from the case when the normal layer is replaced by a superconducting layer from the same material as other layers, i.e., does not differ from a uniform superconductor. Then the ballistic SNS junction is not a weak link, and therefore, there is no Josephson plasma mode with the frequency much lower than the plasma frequency in the superconducting layer and no suppression of the Meisner effect in the normal layer. A weak magnetic field penetrates into the normal layer on the same London penetration depth as into the superconducting layers, in contrast to usual Josephson junctions with the Josephson penetration depth much larger than the London penetration depth. At stronger magnetic fields the Josephson vortices appear with the core size

of the order of the normal layer thickness L . Since their energy is lower than the energy of bulk Abrikosov vortices, Josephson vortices are pinned to the normal layer, and the first critical magnetic field for the SNS junction is smaller than that for superconducting bulk, but not so small as in usual Josephson junctions.

The analysis mostly addresses the 1D case, when only motion along the axis x normal to layers is considered. Its generalization on the 2D and 3D cases is straightforward. Integration over spaces of transverse wave vectors in 2D and 3D cases results in replacement of the 1D electron density by 2D and 3D densities respectively in all expressions for currents, which become current densities.

II. THE BOGOLYUBOV–DE GENNES THEORY

Since in our model the order parameter Δ is supposed to be known we do not need the full BCS Hamiltonian with the interaction term quartic in the electron wave function. It is sufficient to use the quadratic in the wave function second-quantized effective Hamiltonian introduced in the self-consistent field method [14]. Its density is

$$\mathcal{H}_{eff} = \frac{\hbar^2}{2m} [\nabla \hat{\psi}_\gamma^\dagger(x) \nabla \hat{\psi}_\gamma(x) - k_f^2 \hat{\psi}_\gamma^\dagger(x) \hat{\psi}_\gamma(x)] + \Delta \hat{\psi}_\uparrow^\dagger(x) \hat{\psi}_\downarrow^\dagger(x) + \Delta^* \hat{\psi}_\downarrow(x) \hat{\psi}_\uparrow(x), \quad (1)$$

where $\hat{\psi}_\gamma^\dagger(x)$ and $\hat{\psi}_\gamma(x)$ are operators of creation and annihilation of an electron, and the subscript γ has two values corresponding to the spin up (\uparrow) and down (\downarrow). We address a 1D problem with the Fermi wave number k_f , assuming that our system is uniform in the plane normal to the axis x . In multidimensional (2D and 3D) systems with the Fermi wave number k_F $k_f = \sqrt{k_F^2 - k_\perp^2}$, where k_\perp is the transverse component of the multidimensional wave vector \mathbf{k} . The complex order parameter, or gap, Δ can vary in space.

The quadratic effective Hamiltonian can be diagonalized by the Bogolyubov–Valatin transformation from the free electron operators $\hat{\psi}_\gamma^\dagger(x)$ and $\hat{\psi}_\gamma(x)$ to the quasiparticle operators $\hat{a}_{i\gamma}^\dagger$ and $\hat{a}_{i\gamma}$:

$$\begin{aligned} \hat{\psi}_\uparrow(x) &= \sum_i \left[u_i(x) \hat{a}_{i\uparrow} - v_i^*(x) \hat{a}_{i\downarrow}^\dagger \right], \\ \hat{\psi}_\downarrow(x) &= \sum_i \left[u_i(x) \hat{a}_{i\downarrow} + v_i^*(x) \hat{a}_{i\uparrow}^\dagger \right]. \end{aligned} \quad (2)$$

For diagonalization of the effective Hamiltonian the functions $u_i(x)$ and $v_i(x)$ must be stationary solutions of the time-dependent Bogolyubov–de Gennes equations [15]:

$$\begin{aligned} i\hbar \frac{\partial u}{\partial t} &= \frac{\delta \mathcal{H}}{\delta u^*} = -\frac{\hbar^2}{2m} (\nabla^2 + k_f^2) u + \Delta v, \\ i\hbar \frac{\partial v}{\partial t} &= \frac{\delta \mathcal{H}}{\delta v^*} = \frac{\hbar^2}{2m} (\nabla^2 + k_f^2) v + \Delta^* u. \end{aligned} \quad (3)$$

The summation over the subscript i means the summation over all bound and continuum states corresponding to stationary solutions of the Bogolyubov–de Gennes equations Eq. (3). The Bogolyubov–de Gennes equations are the Hamilton equations with the Hamiltonian (per unit volume)

$$\mathcal{H}_{BG} = \frac{\hbar^2}{2m}(|\nabla u|^2 - k_f^2|u|^2) - \frac{\hbar^2}{2m}(|\nabla v|^2 - k_f^2|v|^2) + \Delta u^* v + \Delta^* v^* u. \quad (4)$$

After the diagonalization the effective Hamiltonian becomes

$$\mathcal{H}_{eff} = \sum_i \varepsilon_i (a_{i\uparrow}^\dagger a_{i\uparrow} + a_{i\downarrow}^\dagger a_{i\downarrow} - 2|v|^2), \quad (5)$$

where ε_i is the energy of the i th quasiparticle state.

In general the functions $u(x, t)$ and $v(x, t)$ can be considered as two components of a spinor wave function,

$$\psi(x, t) = \begin{pmatrix} u(x, t) \\ v(x, t) \end{pmatrix}, \quad (6)$$

describing a state of a quasiparticle, which is a superposition of a state with one particle (upper component u) and a state with one antiparticle, or hole (lower component v). The number of particles (charge) is not a quantum number of the state.

The Hamiltonians Eq. (1) and Eq. (4) are not gauge-invariant, and therefore the total number of electrons (charge) is not a conserved quantity. Any i th solution of the Bogolyubov–de Gennes equations Eq. (3) satisfies the continuity equation

$$\frac{\partial n_i}{\partial t} + \frac{1}{e} \nabla j_i = \frac{2i}{\hbar} (\Delta^* v_i^* u_i - \Delta v_i u_i^*), \quad (7)$$

where

$$n_i = |u_i|^2 - |v_i|^2 \quad (8)$$

is the electron density and

$$j_i = -\frac{ie\hbar}{2m} (u_i^* \nabla u_i - u_i \nabla u_i^*) - \frac{ie\hbar}{2m} (v_i^* \nabla v_i - v_i \nabla v_i^*) \quad (9)$$

is the electric current.

Although in the Bogolyubov–de Gennes theory the charge is not conserved, there is another important conservation law for the total probability to find a quasiparticle in the i th state somewhere in the space. The corresponding continuity equation is

$$\frac{\partial \mathcal{N}_i}{\partial t} + \nabla g_i = 0, \quad (10)$$

where

$$\mathcal{N}_i = |u_i|^2 + |v_i|^2 \quad (11)$$

is the quasiparticle density and

$$g_i = -\frac{i\hbar}{2m} (u_i^* \nabla u_i - u_i \nabla u_i^*) + \frac{ie\hbar}{2m} (v_i^* \nabla v_i - v_i \nabla v_i^*) \quad (12)$$

is the current, which will be called the quasiparticle flux. While the density n_i is the difference of the densities of particles and holes, the density \mathcal{N}_i is the sum of these two densities.

The charge conservation law restores if one solves the Bogolyubov–de Gennes equations Eq. (3) together with the self-consistency equation. However, we adopt the approach used earlier [1–3]. Instead of solving the self-consistency equation we simply postulate the gap Δ of constant modulus $\Delta_0 = |\Delta|$ in the superconducting layers and zero gap inside the normal layer. The model is expected to be valid if the thickness L of the normal layer essentially exceeds the coherence length

$$\zeta_0 = \frac{\hbar v_f}{\Delta_0}. \quad (13)$$

The total density n and the total charge current j are expectation values for the operators

$$\begin{aligned} \hat{n}(x) &= \hat{\psi}_\uparrow^\dagger(x) \hat{\psi}_\uparrow(x) + \hat{\psi}_\downarrow^\dagger(x) \hat{\psi}_\downarrow(x) \\ &= \sum_i \left[|u_i(x)|^2 \hat{a}_{i\uparrow}^\dagger \hat{a}_{i\uparrow} + |v_i(x)|^2 \hat{a}_{i\downarrow}^\dagger \hat{a}_{i\downarrow} \right] \\ &= \sum_i \left[|u_i(x)|^2 \hat{a}_{i\uparrow}^\dagger \hat{a}_{i\uparrow} - |v_i(x)|^2 \hat{a}_{i\downarrow}^\dagger \hat{a}_{i\downarrow} + 2|v_i(x)|^2 \right] \end{aligned} \quad (14)$$

$$\begin{aligned} \hat{j} &= -\frac{ie\hbar}{2m} \sum_i \left[(u_i^* \nabla u_i - u_i \nabla u_i^*) \hat{a}_{i\uparrow}^\dagger \hat{a}_{i\uparrow} \right. \\ &\quad \left. + (v_i^* \nabla v_i - v_i \nabla v_i^*) \hat{a}_{i\downarrow}^\dagger \hat{a}_{i\downarrow} - 2(v_i^* \nabla v_i - v_i \nabla v_i^*) \right]. \end{aligned} \quad (15)$$

There are two additive contributions to the density, the energy, and the current [Eqs. (5), (14) and (15) respectively]. One is the vacuum contribution calculated assuming that all energy levels are not occupied (quasiparticle vacuum). This is given by last terms in equations, which do not contain any quasiparticle operator. The other terms in the equations yield the contribution of excitations due to possible occupation of energy levels.

In a resting uniform superconductor with the constant Δ_0 solutions of the Bogolyubov–de Gennes equations are plane waves

$$\begin{pmatrix} u_0 \\ v_0 \end{pmatrix} e^{ik \cdot x - i\varepsilon_0 t / \hbar}, \quad (16)$$

where

$$u_0 = \sqrt{\frac{1}{2} \left(1 + \frac{\xi}{\varepsilon_0} \right)}, \quad v_0 = \sqrt{\frac{1}{2} \left(1 - \frac{\xi}{\varepsilon_0} \right)}. \quad (17)$$

The quasiparticle energy is given by the well known BCS expression

$$\varepsilon_0 = \sqrt{\xi^2 + \Delta_0^2}. \quad (18)$$

Here $\xi = (\hbar^2/2m)(k^2 - k_f^2) \approx \hbar v_f(k - k_f)$ is the quasiparticle energy in the normal Fermi liquid, and $v_f = \hbar k_f/m$

is the Fermi velocity. The states with positive and the negative signs of ξ correspond to particle-like and the hole-like branches of the spectrum respectively. Note that mathematically the Bogolyubov-de Gennes equations have solutions with negative and positive energies $\pm\varepsilon_0$. But only solutions with positive energy ε_0 have the physical meaning [16]. In fact, taking into account solutions with negative energy would be a double-counting since hole-like solutions with positive energy but with $k < k_f$ (negative ξ) have represent all states inside the Fermi surface.

III. BOUND ANDREEV AND CONTINUUM STATES

A. Andreev bound states

The spectrum and the wave function for the present model of the SNS sandwich have been already investigated in previous works, and it is sufficient here to present the resume of these investigations. In the limit of large Fermi wave numbers $k_f \gg \Delta_0/\hbar v_f$ the Bogolyubov-de Gennes equations of the second order in gradients are reduced to the equations of the first order. As a result, the boundary conditions on the interfaces between the normal and superconducting layers require the continuity of the wave function components u and v but not their gradients. The components u and v are superpositions of plane waves with wave numbers close to either only $+k_f$, or only $-k_f$. This means that at interfaces between normal and superconducting layers only Andreev reflection is possible, which does not change the quasiparticle momentum essentially, but the quasiparticle group velocity changes its sign.

Because of Andreev reflection, there are Andreev bound states with energies $0 < \varepsilon_0 < \Delta_0$ localized in the normal layer. The wave functions of these states, which satisfy the Bogolyubov-de Gennes equations and the boundary conditions, are given by

$$\begin{pmatrix} u \\ v \end{pmatrix} = \sqrt{\frac{N}{2}} \begin{pmatrix} e^{\pm \frac{i\eta}{2} \pm \frac{im\varepsilon_0}{\hbar^2 k_f} (x-L/2)} \\ e^{-i\theta_+ \mp \frac{i\eta}{2} \mp \frac{im\varepsilon_0}{\hbar^2 k_f} (x-L/2)} \end{pmatrix} e^{\pm ik_f x} \quad (19)$$

inside the normal layer $-L/2 < x < L/2$,

$$\begin{pmatrix} u \\ v \end{pmatrix} = \sqrt{\frac{N}{2}} \begin{pmatrix} e^{\pm \frac{i\eta}{2}} \\ e^{-i\theta_+ \mp \frac{i\eta}{2}} \end{pmatrix} e^{\pm ik_f x - (x-L/2)/\zeta} \quad (20)$$

inside the superconducting layer at $x > L/2$, and

$$\begin{pmatrix} u \\ v \end{pmatrix} = \sqrt{\frac{N}{2}} \begin{pmatrix} e^{\mp \frac{i\eta}{2}} \\ e^{-i\theta_- \pm \frac{i\eta}{2}} \end{pmatrix} e^{\pm ik_f x + (x+L/2)/\zeta} \quad (21)$$

inside the superconducting layer at $x < -L/2$. Here

$$e^{i\eta} = \frac{\varepsilon_0 + i\sqrt{\Delta_0^2 - \varepsilon_0^2}}{\Delta_0}, \quad \cos \eta = \frac{\varepsilon_0}{\Delta_0}, \quad \sin \eta = \frac{\sqrt{\Delta_0^2 - \varepsilon_0^2}}{\Delta_0}, \quad (22)$$

and θ_+ and θ_- are the constant order parameter phases in the superconducting layers at $x > L/2$ and $x < -L/2$. The upper and lower signs correspond to the wave number semi-spaces $k > 0$ and $k < 0$ respectively. The normalization constant

$$N = \frac{1}{L + \zeta} \quad (23)$$

takes into account the penetration of the bound states into the superconducting layers with the penetration depth

$$\zeta = \zeta_0 \frac{\Delta_0}{\sqrt{\Delta_0^2 - \varepsilon_0^2}}, \quad (24)$$

which diverges when ε_0 approaches to the gap Δ_0 .

The boundary conditions are satisfied at the Bohr-Sommerfeld condition,

$$\varepsilon_0(s, \pm\theta_0) = \frac{\hbar v_f}{2L} (2\pi s + 2\eta \pm \theta_0), \quad (25)$$

which determines the energies of the Andreev states. Here $\theta_0 = \theta_+ - \theta_-$ and s is an arbitrary integer. The notation s for integers will appear further also in other expressions, although its value would be chosen differently. The two signs before θ_0 correspond to positive and negative signs of the 1D wave numbers in the Andreev states. Further we shall call the phase difference θ_0 across the normal layer the bound-state phase, because it shifts the bound states with respect to the gap.

Equation (25) is not an expression but an equation for ε_0 , since η depends on ε_0 . At small energy $\varepsilon_0 \ll \Delta_0$, $\eta = \pi/2$, and the spectrum of the bound states is

$$\varepsilon_0 = \frac{\hbar v_f}{2L} \left[2\pi \left(s + \frac{1}{2} \right) \pm \theta_0 \right]. \quad (26)$$

At the energy ε_0 close to Δ_0 ($\Delta_0 - \varepsilon_0 \ll \Delta_0$) one can use the approximation

$$\eta \approx \sqrt{\frac{2(\Delta_0 - \varepsilon_0)}{\Delta_0}}. \quad (27)$$

Then solution of Eq. (25) for ε_0 yields

$$\varepsilon_0 = \Delta_0 - \frac{\hbar^2 v_f^2}{2\Delta_0 L^2} \left\{ \sqrt{1 + \frac{\Delta_0 L}{\hbar v_f} [2\pi(s + \alpha) \mp \theta_0] - 1} \right\}^2, \quad (28)$$

where α is the fractional part of the ratio

$$\frac{\Delta_0 L}{\pi \hbar v_f} = s + \alpha. \quad (29)$$

An integer s is chosen so that $0 < \alpha < 1$. The parameter α is the measure of incommensurability of the gap Δ_0 with the level energy spacing.

The charge current in the occupied s th Andreev state is determined by the canonical relation

$$j_{\pm}(s) = \frac{2e}{\hbar} \frac{\partial \varepsilon_0(s, \pm \theta_0)}{\partial \theta_0} = \pm \frac{ev_f}{L + \zeta}. \quad (30)$$

The factor 2 takes into account that θ_0 is the phase of a Cooper pair but not of a single electron. As expected, this expression fully agrees with the fact that the mass current is the total momentum $\hbar k_f$ in the state divided by the size $L + \zeta$ of the bound state.

The existence of charge current in a bound state is the consequence of the absence of the charge conservation law in our model. At the same time, the quasiparticle flux given by Eq. (12) vanishes in accordance with the conservation law Eq. (10) for the total number of quasiparticles.

B. Continuum states

Delocalized continuum states with $\varepsilon_0 > \Delta_0$ are scattering states. For a quasiparticle ($\xi > 0$) incident from left and propagating from $x = -\infty$ to $x = \infty$ the wave function is

$$\begin{aligned} & \begin{pmatrix} u_0(\xi) \\ v_0(\xi)e^{-i\theta_-} \end{pmatrix} e^{i\left(k_f + \frac{m\xi}{\hbar^2 k_f}\right)x} \\ & + r \begin{pmatrix} u_0(-\xi) \\ v_0(-\xi)e^{-i\theta_-} \end{pmatrix} e^{i\left(k_f - \frac{m\xi}{\hbar^2 k_f}\right)x} \end{aligned} \quad (31)$$

for $x < -L/2$, and

$$t \begin{pmatrix} u_0(\xi) \\ v_0(\xi)e^{-i\theta_+} \end{pmatrix} e^{i\left(k_f + \frac{m\xi}{\hbar^2 k_f}\right)x} \quad (32)$$

for $x > L/2$. Here t and r are amplitudes of transmission and reflection determined from the continuity of spinor components at $x = \pm L/2$ [3]. As in the case of bound states, the analysis considers only the Andreev reflection. The reflection and the transmission probabilities are

$$R(\theta_0) = |r|^2 = \frac{\Delta_0^2 \left[1 - \cos\left(\frac{2\varepsilon_0 m L}{\hbar^2 k_f} - \theta_0\right)\right]}{2\varepsilon_0^2 - \Delta_0^2 - \Delta_0^2 \cos\left(\frac{2\varepsilon_0 m L}{\hbar^2 k_f} - \theta_0\right)}, \quad (33)$$

$$\mathcal{T}(\theta_0) = |t|^2 = \frac{2(\varepsilon_0^2 - \Delta_0^2)}{2\varepsilon_0^2 - \Delta_0^2 - \Delta_0^2 \cos\left(\frac{2\varepsilon_0 m L}{\hbar^2 k_f} - \theta_0\right)}. \quad (34)$$

The spinor in the normal layer $-L/2 < z < L/2$ is given by the same expression as Eq. (19) for the bound state, but with different normalization constant $N = \mathcal{T}$.

Similar expressions with the same $R(\theta_0)$ and $\mathcal{T}(\theta_0)$ can be derived for a quasihole ($\xi < 0$) incident from right and moving to left. For a quasiparticle incident from right and a hole incident from left the reflection and the transmission probabilities are $R(-\theta_0)$ and $\mathcal{T}(-\theta_0)$.

The transmission probability differs from unity in the energy interval of the order Δ_0 small with respect to the Fermi energy $\varepsilon_f = \hbar^2 k_f^2 / 2m$. The condition $R + \mathcal{T} = 1$ follows from the conservation law for the number of quasiparticles, which leads to the constant quasiparticle flux g in the whole space [see Eq. (12)]. The scattering delocalized states in the SNS sandwich were determined for $\theta_0 = 0$ by Bardeen and Johnson [3] and for $\theta_0 \neq 0$ in Refs. 17 and 18.

One can transform expressions for R and \mathcal{T} demonstrating their dependence on the incommensurability parameter α introduced in Eq. (29):

$$\mathcal{T} = \frac{2(\varepsilon_0^2 - \Delta_0^2)}{2\varepsilon_0^2 - \Delta_0^2 - \Delta_0^2 \cos\left[\frac{2(\varepsilon_0 - \Delta_0)mL}{\hbar^2 k_f} + 2\pi\alpha - \theta_0\right]}. \quad (35)$$

The reflection probability can be transformed similarly. The both probabilities rapidly oscillate as functions of the energy, and at large L one may average over these oscillations neglecting variation of the energy ε_0 within the short oscillation period. The averaged reflection probability is

$$\begin{aligned} \bar{\mathcal{T}} &= \frac{1}{2\pi} \int_{-\pi}^{\pi} \frac{2(\varepsilon_0^2 - \Delta_0^2)d\phi}{2\varepsilon_0^2 - \Delta_0^2 - \Delta_0^2 \cos \phi} \\ &= \frac{2(\varepsilon_0^2 - \Delta_0^2)}{\sqrt{(2\varepsilon_0^2 - \Delta_0^2)^2 - \Delta_0^4}} = \frac{\sqrt{\varepsilon_0^2 - \Delta_0^2}}{\varepsilon_0}. \end{aligned} \quad (36)$$

After averaging neither the incommensurability parameter α , nor the phase θ_0 influence contributions of continuum states to the transport process.

IV. THE GROUND STATE (QUASIPARTICLE VACUUM)

A. Vacuum current

In the ground state in the superconducting layers the electron fluid is at rest, and there are no currents. Mathematically in our model the bound-state phase θ_0 is an independent parameter, and the energy of Andreev states depends on it. In order to determine the ground state, one should find the θ_0 -dependent energy of Andreev states and minimize it with respect to θ_0 . Since the charge current is determined by the derivative of the energy with respect to θ_0 , after minimization the current vanishes as it should be in the ground state.

Further we consider the vacuum not in the ground state when the current does not vanish. Frequently the terms “vacuum” and “ground state” are considered as synonyms. But we define vacuum as a broader term meaning the quasiparticle vacuum when all Andreev levels are empty.

Neglecting the penetration depth ζ in Eq. (30), the total current of all bound states vanishes if the numbers of states with positive and negative momenta [two signs

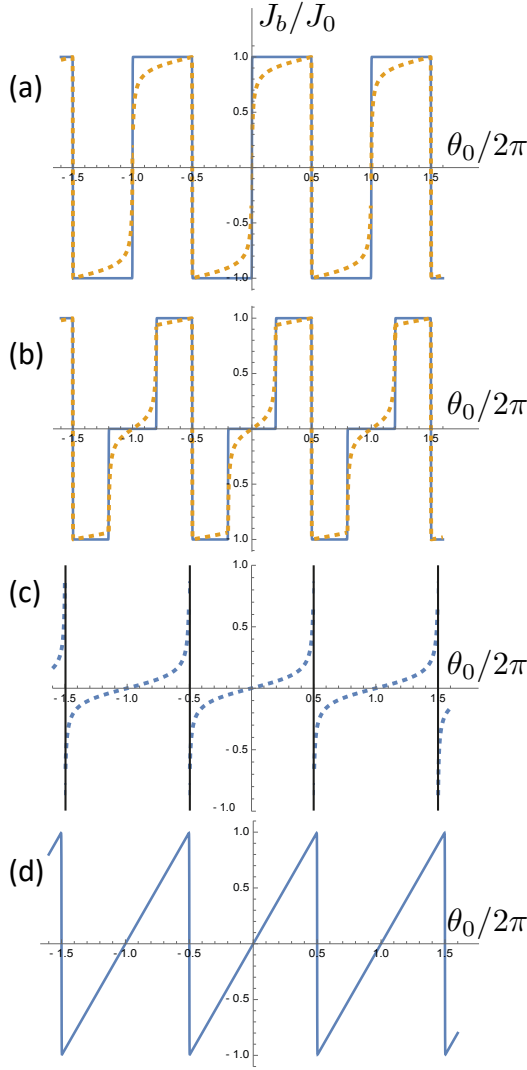


FIG. 2. The vacuum current and energy vs. the bound-state phase θ_0 . Currents calculated neglecting or taking into account penetration of Andreev states into superconducting layers at $L/\zeta_0 = 50$ are shown by solid and dashed lines respectively. The plots for α and $1 - \alpha$ are identical. (a) $\alpha = 0$. (b) $\alpha = 0.2$. (c) The current and the energy averaged over α .

in Eq. (30)] are equal (the sum of the numbers of states is even), and they cancel one another. This is the case at phases $\theta_0 = 0$ and $\theta_0 = \pm\pi$. However, at tuning the phase θ_0 energy levels move. At the both edges of the Andreev energy spectrum $\varepsilon_0 = 0$ and $\varepsilon_0 = \Delta_0$ some levels can exit from the gap and some new levels can enter it. If $\alpha = 1/2$ the entrance and the exit processes at the two edges are synchronized: at $\theta_0 = \pm\pi$ a level exits (enters) at the lower edge $\varepsilon_0 = 0$ [see Eq. (26)] and simultaneously a level enters (exits) at the upper edge $\varepsilon_0 = \Delta_0$ [see Eq. (28)]. The numbers of states with positive and negative momenta remain equal, and the total current vanishes. At $\alpha \neq 1/2$ levels enter or exit at the lower edge of the Andreev spectrum at $\theta_0 =$

$\pm\pi$ as before, but levels cross the upper edge at $\theta_0 = \pm 2\pi\alpha$. At $-\pi < \theta_0 < -2\pi\alpha$ and $\pi > \theta_0 > 2\pi\alpha$ there is one state with a positive or negative momentum without its counterpart with an opposite-sign momentum. This means that the total momentum is $\pm\hbar k_f$ and the total electric current is $\pm ev_f/L$. Eventually the total vacuum current is

$$J_v = - \sum_s [j_+(s) + j_-(s)] = J_0 \sum_s \{H[\theta - 2\pi(s + \alpha)] + H[\theta - 2\pi(s + 1 - \alpha)] - 2H(\theta - 2\pi s - \pi)\}, \quad (37)$$

where $H(q)$ is the Heaviside step function and

$$J_0 = \frac{ev_f}{L} = \frac{\pi e \hbar n_0}{2mL}. \quad (38)$$

Deriving Eq. (37) we took into account that at any s and sign of θ there are two states corresponding to two spin values and that according to Eq. (15) the vacuum current at an Andreev state is two times less and has an opposite sign than the quasiparticle current $j_{\pm}(s)$. The factors 2 and 1/2 cancel one another.

In Eq. (38) the relation $k_f = \pi n_0/2$ between k_f and the 1D electron density n_0 was used. After this substitution the formula becomes valid also for 2D and 3D systems bearing in mind that at this generalization n_0 and J_v become the electron density and current density in 2D and 3D systems respectively.

The stepwise dependence of the current J_v on the phase θ_0 at various α is shown in Figs. 2(a)–(d) by solid lines. At $\alpha = 1/2$ when the Andreev levels cross the lower ($\varepsilon_0 = 0$) and the upper ($\varepsilon_0 = \Delta_0$) edge of the gap synchronically the vacuum current vanishes except for the phases $\theta_0 = 2\pi(s + \frac{1}{2})$. At these phases the vacuum current is proportional to the derivative of the δ -function $\delta[\theta_0 - 2\pi(s + \frac{1}{2})]$.

In our derivation of the vacuum current dependence on θ_0 we used the concept of the spectral flow, which is rather popular in the analysis of SNS junctions (see, e.g., Refs. 19 and 20). The concept assumes that tuning of the phase θ_0 leads to steady motion of Andreev levels, which cross the whole gap, i.e., enter the gap on one gap edge and exit from the gap on the other edge. However, this picture is valid only in the limit of infinite Fermi wave number when the Andreev level are degenerate at the phases 0 and π . Even small corrections to this limit lift this degeneracy introducing small gaps at the phases 0 and π . As a result, at phase tuning the Andreev levels do not cross the gap but oscillate within bands separated by the aforementioned small gaps. Our conclusions remain valid even after this modification of topology of Andreev levels. This illustrated in Fig. 3 for the case $\alpha = 0$ shown in Fig. 2(a). Figure 3 shows the variation of the Andreev-level energies with varying phase θ_0 . In shaded part of the spectrum at any phase the numbers of levels with positive and negative slope (i.e., with positive and negative currents) coincide. Thus, contributions of these levels to the total vacuum current vanish. The variation of the total vacuum current with the phase is determined only

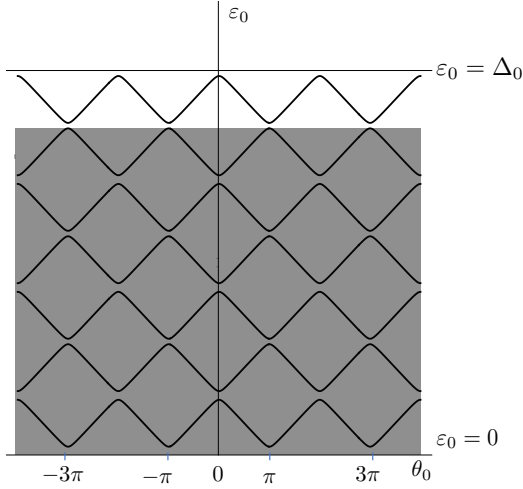


FIG. 3. The Andreev spectrum variation at tuning the bound-state phase θ_0 at $\alpha = 0$. In the shaded area the number of Andreev states with energies growing and decreasing with θ_0 are equal and the total current in these states vanishes (see the text). Only the unshaded band closest to the gap edge $\varepsilon_0 = \Delta_0$ is responsible for the total current periodical dependence on θ_0 .

by the contribution of the unshaded band closest to the gap edge. This contribution (taking into account that for any Andreev state the vacuum current differs from the current of the occupied state by the factor $-1/2$) coincides with that shown by a solid line in Fig. 2(a).

The periodic dependence of the current on the incommensurability parameter is fragile. In 2D and 3D systems integration over the transverse components of the wave vectors should wipe out this dependence. So, it is reasonable to consider the current averaged over α in the interval from 0 to 1. After averaging the vacuum current in the interval $-\pi < \theta_0 < \pi$ is

$$J_v = J_0 \frac{\theta_0}{\pi}. \quad (39)$$

The periodical saw-tooth dependence of the current J_v on θ_0 is shown in Fig. 2(c).

However, the penetration depth ζ diverges at $\varepsilon_0 \rightarrow \Delta_0$. According to Eq. (30), at $\zeta \rightarrow \infty$ the current in the bound state crossing the upper gap edge vanishes. Therefore, we performed a more accurate calculation in this limit. At $\Delta_0 - \varepsilon_0 \ll \Delta_0$ the spectrum of bound state is described by Eq. (28), and the total current in all bound states is

$$J_v = -\frac{J_0}{2} \left\{ \left[1 - \frac{1}{\sqrt{1 + \frac{\Delta_0 L}{\hbar v_f} (2\pi\alpha - \theta_0)}} \right] H(2\pi\alpha - \theta_0) - \left[1 - \frac{1}{\sqrt{1 + \frac{\Delta_0 L}{\hbar v_f} (2\pi\alpha + \theta_0)}} \right] H(2\pi\alpha + \theta_0) \right. \\ \left. + \zeta \left(\frac{1}{2}, \frac{\hbar v_f}{2\pi\Delta_0 L} + 1 + \alpha - \frac{\theta_0}{2\pi} \right) - \zeta \left(\frac{1}{2}, \frac{\hbar v_f}{2\pi\Delta_0 L} + 1 + \alpha + \frac{\theta_0}{2\pi} \right) \right\}. \quad (40)$$

Here

$$\zeta(z, q) = \sum_{s=0}^{\infty} \frac{1}{(q+s)^z} \quad (41)$$

is Riemann's zeta function [21]. The series for Riemann's zeta function at $z = 1/2$ diverges, but the series for a difference of zeta functions with different arguments q converges at large s , which, nevertheless, correspond to energies satisfying the condition $\Delta_0 - \varepsilon_0 \ll \Delta_0$. Therefore, one can use the infinite series with $s \rightarrow \infty$. The vacuum current J_v calculated taking into account penetration of Andreev states into superconducting layers at $L/\zeta_0 = 50$ is shown in Fig. 2(a)–(c) by dashed lines. Summarizing, the divergence of the penetration depth at $\varepsilon_0 \rightarrow \Delta_0$ smears the current jump at crossing of the gap edge $\varepsilon_0 = \Delta_0$ by the Andreev level transforming it into a smooth crossover. But the width of the crossover is small compared to the distance between levels and can be ignored in the limit $L \rightarrow \infty$.

B. Vacuum density

In the ballistic regime the boundary conditions on the interface affect the wave function in the whole bulk, but it is natural to expect that the average density in the vacuum in the ballistic and the diffusive regime do not differ and are fully determined by the volume of the Fermi sphere as Luttinger's theorem [22] states. This also follows from the principle that although dissipative processes are necessary for relaxation to the ground state, the final ground state itself is not determined by these processes. Nevertheless, it is useful to check this principle for the SNS sandwich, although this is a check of our analysis rather than of the principle itself.

In the superconducting layers at $x < -L/2$ and $x > L/2$ all states are delocalized and form the continuum. For the determination of the vacuum particle density one can replace in Eq. (14) summation by integration, and the total vacuum density for two spins and all possible directions of motion of incident quasiparticles and quasi-

holes is

$$n_0 = \frac{1}{\pi} \int_{-\infty}^{\infty} |v|^2 dk = \frac{1}{\pi \hbar v_f} \int_{-\infty}^{\infty} |v|^2 d\xi, \quad (42)$$

where

$$|v|^2 = \frac{|v_0|^2}{4} [2 + R(\theta_0) + \mathcal{T}(\theta_0) + R(-\theta_0) + \mathcal{T}(-\theta_0)] = |v_0|^2 = \frac{1}{2} \left(1 - \frac{\xi}{\varepsilon_0} \right). \quad (43)$$

The value of n_0 coincides with the density $n_0 = 2k_f/\pi$ in a uniform superconductor. So, scattering does not affect the average density n_0 in the superconducting layers.

We start the estimation of the density in the normal layer $-L/2 < x < L/2$ from the contribution of the Andreev bound states. Any bound state is a superposition of a particle state and of a hole state with equal probability 1/2. Thus, in the normal layer the contribution of Andreev states to the vacuum density is simply a half of the number of bound states per unit length:

$$n_{0b} = \frac{2k_f}{\pi} \frac{\Delta_0}{\varepsilon_f} = n_0 \frac{\Delta_0}{\varepsilon_f}. \quad (44)$$

The contribution of the continuum states in the normal layer is

$$n_{0c} = \frac{1}{\pi \hbar v_f} \int_{-\infty}^{\infty} |v|^2 \bar{\mathcal{T}} d\xi = n_0 \left(1 - \frac{\Delta_0}{\varepsilon_f} \right). \quad (45)$$

The averaged transmission probability $\bar{\mathcal{T}}$ is given by Eq. (36). Together with the contribution Eq. (44) the total density $n_0 = n_{0b} + n_{0c}$ is the same as in uniform normal metals or superconductors with the Fermi energy ε_f .

V. MOVING COOPER PAIR CONDENSATE

A. Effect of the Cooper pair condensate motion on Andreev states (Doppler shift)

Let us consider the case of the moving Cooper pair condensate when in the superconducting layers there is an order parameter phase gradient $\nabla\varphi$, which determines the superfluid velocity v_s :

$$v_s = \frac{\hbar}{2m} \nabla\varphi. \quad (46)$$

We must solve the Bogolyubov-de Gennes equations Eq. (3) with the gap

$$\Delta = \begin{cases} \Delta_0 e^{i\theta_+ + i\nabla\varphi x} & x > L/2 \\ 0 & -L/2 < x < L/2 \\ \Delta_0 e^{i\theta_- + i\nabla\varphi x} & x < -L/2 \end{cases}. \quad (47)$$

The solution differs from the solution Eqs. (19)–(21) obtained for the resting condensate by the presence of the

additional factors $e^{imv_s x/\hbar}$ and $e^{-imv_s x/\hbar}$ in the expressions for the components u and v respectively. These factors are cancel in the boundary conditions, and the expressions for ε_0 [Eqs. (25), (26) and (28)] and for the reflection and transmission probabilities [Eqs. (33)–(35)] remains valid. However, the energy ε of an Andreev state differs from ε_0 by the Doppler shift:

$$\varepsilon(s, \pm\theta_0) = \varepsilon_0(s, \pm\theta_0) \pm v_s k_f. \quad (48)$$

In particular, at low energies $\varepsilon_0 \ll \Delta_0$

$$\varepsilon(s, \pm\theta_0) = \frac{\hbar v_f}{2L} \left[2\pi \left(s + \frac{1}{2} \right) \pm (\theta_0 + \theta_s) \right], \quad (49)$$

where

$$\theta_s = \frac{2mLv_s}{\hbar} \quad (50)$$

is the phase difference across the normal layer as if it were not normal but superconducting (Fig. 1). Therefore, further it will be called superfluid phase.

According to Eq. (49), the effects of the bound-state phase θ_0 and the superfluid phase θ_s on the energy are

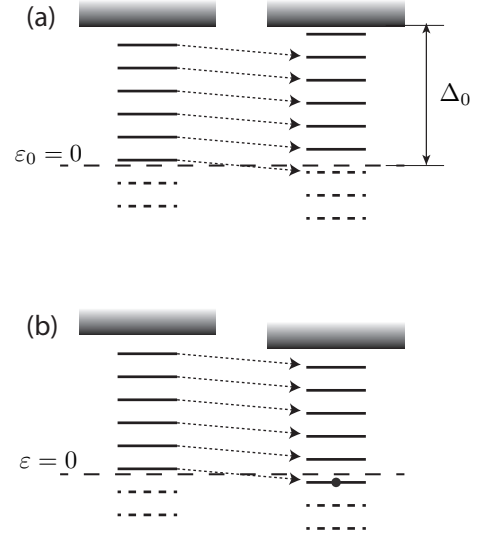


FIG. 4. Tuning of the energies of the Andreev states by the phases θ_0 and θ_s . Horizontal solid lines show unoccupied Andreev levels. A horizontal solid line with a black circle shows an occupied Andreev level. Horizontal dashed lines show ghost levels with negative ε_0 , which correspond to mathematical correct solutions of the Bogolyubov-de Gennes equations, but are not considered in the BCS theory as physically real bound states. Arrowed dashed lines show shifts of levels by tuning the phases θ_0 and θ_s . (a) Tuning by the phase θ_0 at constant θ_s . The lowest physical level crosses the energy $\varepsilon_0 = 0$ and transforms to a ghost level, i.e., disappears. (b) Tuning by the phase θ_s at constant θ_0 . All levels move together with the gap edge with the energy ε_0 remained constant. The lowest physical level crosses the energy $\varepsilon = 0$ and becomes occupied even at zero temperature.

additive, and the energy depends only on their sum. But it is true as far as θ_s (velocity v_s) is small. In general, there is an essential difference between effects of θ_0 and θ_s on the Andreev spectrum. We saw that variation of θ_0 makes the Andreev levels to move with respect to the Andreev spectrum edges. As a result, some new levels can emerge and some old ones can disappear. In contrast, variation of θ_s leads to the shift of the Andreev spectrum as a whole without changing positions of levels with respect to the Andreev spectrum edges. This is illustrated in Fig. 4. The principle of the BCS theory that only solutions with positive energies should be taking into account refers to the energy ε_0 , while the Doppler-shifted energy ε can be both positive or negative. If ε is negative the level is occupied at zero temperature. This is important for the further analysis.

B. Charge currents due to the motion of the Cooper pair condensate

The expression for the charge current J_s produced by the moving Cooper pair condensate follows from Eq. (15), in which only the vacuum contribution is taken into account:

$$J_s = \frac{ie\hbar}{m} \sum_i (v_i^* \nabla v_i - v_i \nabla v_i^*), \quad (51)$$

where summation is over all bound and continuum states, but the summation over continuum states can be replaced by integration. Comparing this expression with the vacuum contribution to the electron density in Eq. (14) one can see that the motion of the Cooper pair condensate produces the θ_s -dependent charge current

$$J_s = en_0 v_s = J_0 \frac{\theta_s}{\pi}, \quad (52)$$

in all layers of the sandwich as in a uniform superconductor [3]. Thus, the condensate motion induces charge currents satisfying the charge conservation law even in the absence of vacuum and excitation currents in Andreev bound states. This contrasts with the vacuum current, which is produced by the bound-state phase θ_0 only in the normal layer and must be compensated by the excitation current in order to satisfy the charge conservation law.

VI. EXCITATION CONTRIBUTION TO THE CURRENT

Andreev levels in the SNS sandwich are occupied at finite temperatures or even at zero temperature if the energy ε of some Andreev levels becomes negative due to the Doppler shift. We consider only temperatures much lower than the gap Δ_0 . So quasiparticles in the superconducting layers are absent. But the temperature can be on the order or higher than the energy distance between

Andreev levels. The contribution of excitations (quasi-particles occupying Andreev levels) to the current at the temperature T is

$$J_q = 2J_0 \sum_s \left[\frac{H(s + 1/2 + \theta_0/2\pi)}{e^{\beta(s+1/2+\theta/2\pi)} + 1} - \frac{H(s + 1/2 - \theta_0/2\pi)}{e^{\beta(s+1/2-\theta/2\pi)} + 1} \right], \quad (53)$$

where $\theta = \theta_s + \theta_0$ and

$$\beta = \frac{\pi\hbar v_f}{LT}. \quad (54)$$

The Heaviside functions in numerators provide that only states of the Andreev spectrum with $\varepsilon_0 > 0$ contribute to the current. At zero temperature ($\beta \rightarrow \infty$) the Fermi distribution function also becomes the Heaviside function, and the excitation current is

$$J_q = -\frac{\theta_s}{|\theta_s|} 2J_0 \quad (55)$$

in the interval

$$2\pi \left(s + \frac{1}{2} \right) - \theta_s < \theta_0 < 2\pi \left(s + \frac{1}{2} \right). \quad (56)$$

At high temperatures ($\beta \rightarrow 0$) the summation in Eq. (53) can be replaced by integration. In the interval $|\theta_s|, |\theta_0| < \pi$:

$$J_q \approx 2J_0 \int_0^\infty \left[\frac{ds}{e^{\beta(s+\theta/2\pi)} + 1} - \frac{ds}{e^{\beta(s-\theta/2\pi)} + 1} \right] = -J_0 \frac{\theta}{\pi}. \quad (57)$$

The contribution of quasiparticles at occupied Andreev states to the current is shown in Fig. 5 for $\beta \rightarrow \infty$ (zero temperature), $\beta = 30$ (low temperature), and $\beta \rightarrow 0$ (high temperature) by the solid, dashed, and dotted line respectively.

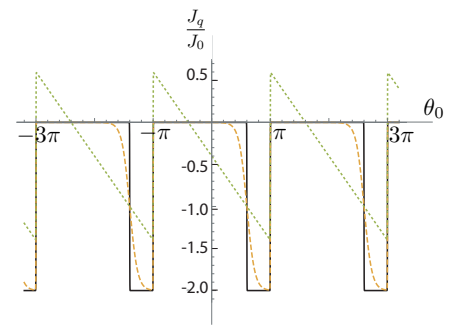


FIG. 5. The excitation current vs. the bound-state phase θ_0 at $\theta_s = 0.4\pi$. Solid, dashed, and dotted lines show the current at zero temperature ($\beta \rightarrow \infty$), low temperature ($\beta = 30$), and high temperature ($\beta \rightarrow 0$) respectively.

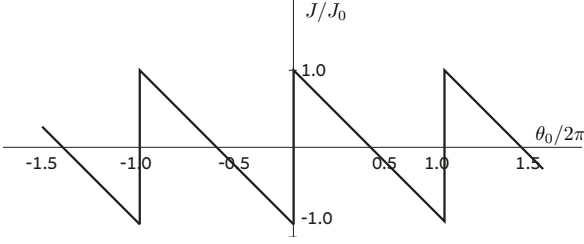


FIG. 6. The current–phase θ_0 relation for zero temperature.

VII. CHARGE CONSERVATION LAW AND CURRENT–PHASE RELATION

As already mentioned, our model does not satisfy the charge conservation law, and stationary solutions of the model with different currents in different layers are mathematically correct. However, only solutions, which *do satisfy* the charge conservation law, have a physical meaning and must be chosen. One can meet this requirement by imposing the condition that in the stationary case the current in the normal layer does not differ from the current in the superconducting layers. Since the motion of the condensate with the velocity v_s produces the same current J_s in all layers, the vacuum and excitation currents J_v and J_q in Andreev states must cancel one another: $J_v + J_q = 0$. So, the total current $J = J_v + J_q + J_s$ cannot differ from J_s .

Figure 6 shows the current–phase θ_0 relation obtained from the condition $J_v + J_q = 0$ at zero temperature. It is remarkable that at zero temperature the current–phase curve $J(\theta_0)$ does not depend on the incommensurability parameter α . Along vertical segments of the curve at $\theta_0 = 2\pi s$ both J_v and J_q vanish and all Andreev levels are unoccupied. Compensation of a nonzero vacuum current at $\theta_0 \neq 2\pi s$ by an excitation current is possible if the lowest-energy Andreev level reaches zero and is at least partially occupied. According to Eq. (26), this takes place if $\theta_0 + \theta_s = 2\pi(s + \frac{1}{2})$. Using Eq. (52) one obtains the current

$$J = J_s = \frac{J_0}{\pi} (2\pi s + \pi - \theta_0). \quad (58)$$

at the sloped segments of the current–phase curve in Fig. 6, which does not depend on the incommensurability parameter α . Independence from α makes averaging over α in 2D and 3D systems unnecessary. Thus, the current–phase curve shown in Fig. 6 is valid for a system of any dimensionality at zero temperature.

But at finite temperature the current–phase relation *does depend* on α . The current–phase curve $J_v(\theta_0)$ at high temperature is shown in Fig. 7 for $\alpha = 0$, $\alpha = 0.2$, and $\alpha = 1/2$. For $\alpha = 0$ the current–phase curve $J_v(\theta_0)$ at high temperature does not differ from that at zero temperature shown in Fig. 6.

The α -dependent current–phase curves in Fig. 7 are valid only in the 1D case. After averaging over α in the

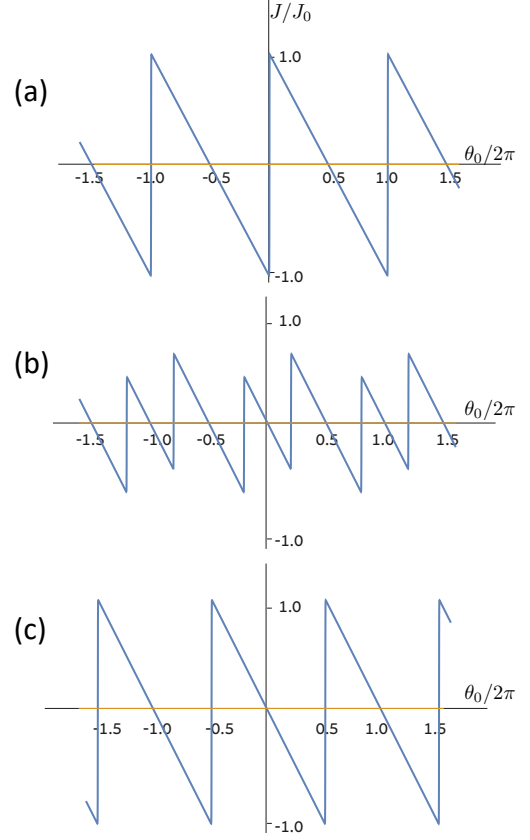


FIG. 7. The current–phase θ_0 relation for high temperature. (a) $\alpha = 0$. (b) $\alpha = 0.2$. (c) $\alpha = 1/2$.

multidimensional (2D and 3D) systems the vacuum current J_v given by Eq. (39) can compensate the excitation current J_q [Eq. (57)] only at $\theta_s = 0$. So, the supercurrent vanishes in the limit of high temperature when summation in the expression Eq. (53) can be replaced by integration. At temperature not high enough for validation of this approximation the supercurrent does not vanish completely but strongly decreases with temperature.

However, the bound-state phase θ_0 is not a phase, which must be used in the canonical description of the Josephson junction by the pair of conjugate variables “charge–phase”. The proper phase is the total phase difference across the normal layer $\theta = \theta_0 + \theta_s$, which we call Josephson phase (Fig. 1). The time derivative of the phase θ determines the voltage drop across the normal layer:

$$V = \frac{\hbar}{2e} \frac{d\theta}{dt}. \quad (59)$$

Figure 8 shows the current–phase relation for the Josephson phase θ at various values of α at high temperature. In the phase interval $(-\pi, \pi)$ it is given by

$$J(\theta) = J_0 \left(\frac{\theta}{\pi} - 2\alpha \frac{\theta}{|\theta|} \right). \quad (60)$$

The critical Josephson current (its maximum value) depends on α :

$$J_c = J_0 \times \begin{cases} 1 - 2\alpha & \alpha < \frac{1}{4} \\ 2\alpha & \alpha > \frac{1}{4} \end{cases}. \quad (61)$$

According to Fig. 8, at any nonzero α the current at small positive (negative) θ becomes negative (positive). This means that at $\alpha \neq 0$ the Josephson energy

$$E_J = \frac{\hbar}{2e} \int_{-\pi}^{\pi} J(\theta) d\theta, \quad (62)$$

has not a minimum but a maximum. The energy minimum (ground state) is at the phase $\theta = 2\pi\alpha$. At varying α from 0 [Fig. 8(a)] to $1/2$ [Fig. 8(d)] the phase θ in the ground state varies from 0 to π . The case $\theta = \pi$ corresponds to a π junction well known in the past (see Introduction). In general, one can call junctions with the nonzero θ in the ground state θ junctions. The current-phase curve of the $\pi/2$ junction ($\alpha = 1/4$) in Fig. 8(c) is periodical with the period π instead of 2π and the critical current has a minimum, which is two times smaller than that for 0 and π junction ($\alpha=0$ or $1/2$).

The current-phase relation shown in Fig. 8(a), which is valid for $\alpha = 0$ for 1D systems at high temperature and for any α and any dimensionality at zero temperature, does not differ from the current-phase relation obtained by Bardeen and Johnson [3] at zero temperature. Our analysis of multidimensional (2D and 3D) systems also confirms their conclusion that the supercurrent vanishes in the limit of temperatures much higher than the Andreev level energy spacing. However, our physical picture of the phenomenon differs from theirs. Bardeen and Johnson [3] took into account the current J_s produced by the condensate motion and the excitation current J_q , but ignored the vacuum current J_v determined by the phase θ_0 absent in their analysis. The charge conservation law requires that the sum J_v and J_q must vanish. The analysis of Ref. 3 does not meet this requirement. The difference between the physical pictures is important for 1D systems at high temperatures. In this case suppression of the supercurrent at high temperature predicted by Bardeen and Johnson [3] is not valid.

VIII. SOME PROPERTIES OF THE SNS SANDWICH AS A JOSEPHSON JUNCTION

A. The nonstationary Josephson effect at current bias

Let us consider the SNS sandwich shunted by ohmic resistance R at the current bias I exceeding the critical one. The general expression for the average voltage for the overdamped Josephson junction is [16]

$$\bar{V} = \frac{2\pi R}{\int_{-\pi}^{\pi} \frac{d\theta}{I - J(\theta)}}. \quad (63)$$

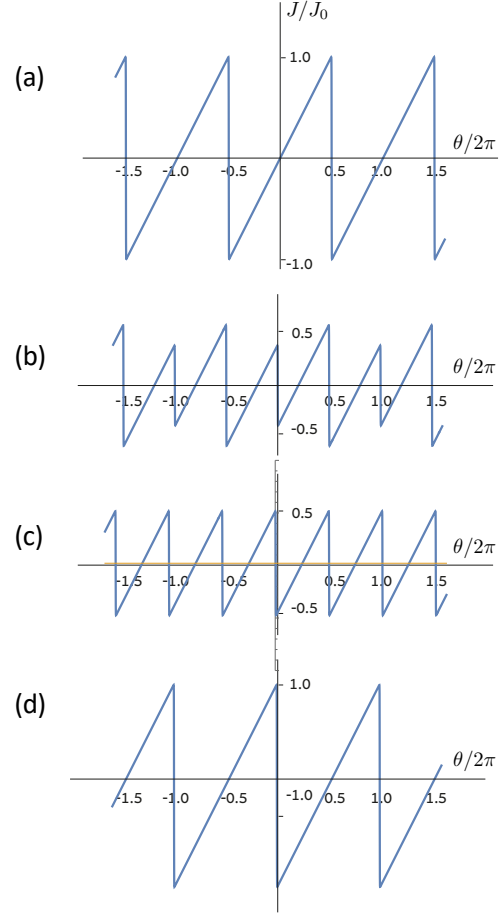


FIG. 8. The current-phase θ relation for high temperature. (a) $\alpha = 0$. The same curve describes the current-phase relation at zero temperature, which is independent from α . (b) $\alpha = 0.2$. (c) $\alpha = 0.25$. (d) $\alpha = 1/2$.

For the current-phase relations at high temperature shown in Fig. 8 this yields the VI curve

$$\bar{V} = \frac{2RJ_0}{\ln \frac{(I+2\alpha J_0)[I+(1-2\alpha)J_0]}{(I-2\alpha J_0)[I-(1-2\alpha)J_0]}}. \quad (64)$$

Using the expression Eq. (61) for the critical current one obtains

$$\bar{V} = 2RJ_c \times \begin{cases} \frac{1}{\ln \frac{[(1-2\alpha)I+2\alpha J_c](I+J_c)}{[(1-2\alpha)I-2\alpha J_c](I-J_c)}} & \alpha < \frac{1}{4} \\ \frac{1}{\ln \frac{[2\alpha I+(1-2\alpha)J_c](I+J_c)}{[2\alpha I-(1-2\alpha)J_c](I-J_c)}} & \alpha > \frac{1}{4} \end{cases}. \quad (65)$$

We remind that for $\alpha = 0$ the current-phase relations at zero and high temperature do not differ, and the VI curve is

$$\bar{V} = \frac{2RJ_c}{\ln \frac{I+J_c}{I-J_c}}. \quad (66)$$

All curves follow the Ohm law $\bar{V} = RI$ at $I \gg J_c$. We note for comparison that for Josephson junctions with

the sinusoidal current–phase relation the VI curve is $\bar{V} = R\sqrt{I^2 - J_c^2}$ [16].

B. The Josephson plasma mode. Is the SNS sandwich always a weak link?

Although the dynamical analysis is beyond the scope of the present work, we still want to address the first elementary step of this analysis: the small oscillation around the ground state. For the Josephson junction this is the Josephson plasma oscillation. For an arbitrary current–phase relation the Josephson plasma frequency is given by

$$\omega_J = \sqrt{\frac{2e}{C\hbar} \frac{dJ(\theta)}{d\theta}}, \quad (67)$$

where C is the capacitance of the Josephson junction and the derivative $dJ(\theta)/d\theta$ is taken at θ , which corresponds to the ground state. In usual Josephson junctions the Josephson plasma frequency is much lower than the plasma frequency

$$\omega_0 = \sqrt{\frac{4\pi e^2 n_0}{m}} \quad (68)$$

in the bulk superconductor. This inequality is in fact a necessary condition for the existence of the Josephson plasma mode localized at the Josephson junction and decaying inside the superconducting bulk.

Now let us consider a 3D sandwich, which is a planar Josephson SNS junction when the capacitance C and the current $J(\theta)$ can be replaced by the capacity $4\pi/L$ per unit area and the current density $J(\theta)/S$, where S is the area in the junction plane. At zero temperature (more generally, at temperature much lower than the Andreev level energy spacing), the SNS sandwich near the ground state is in the regime of pure condensate charge transport, in which the vacuum and the excitation currents are absent, $\theta = \theta_s$, and according to Eq. (52), $dJ(\theta)/d\theta = dJ_s(\theta_s)/d\theta_s = J_0/\pi$. Then ω_J and ω_0 coincide. Thus, there is no localized Josephson plasma mode.

The localized Josephson plasma mode in a Josephson junction exists because the junction is a weak link. The hallmark of weak link is that the supercurrent through the junction requires a phase gradient (ratio of the phase difference across the junction to its length) much larger than the phase gradient providing the same current in the bulk superconductor. The ballistic SNS sandwich at zero temperature is not a weak link in this meaning.

C. Meissner effect and Josephson vortices

Another manifestation that due to the incommensurability effect the SNS sandwich is not always a weak link is its response to a weak magnetic field (Meissner effect). In the case of a usual planar Josephson junction

the magnetic field penetrates along the junction plane on the Josephson penetration depth, which is much longer than the London penetration depth into the superconducting bulk. A planar ballistic SNS junction at zero temperature is not a weak link, and in the normal layer a supercurrent is supported by the same phase gradient as in superconducting layers. Therefore, the Josephson penetration depth does not differ from the London penetration depth.

Despite the SNS sandwich is not a weak link with respect to linear effects like the Josephson plasma oscillation or the Meissner effect, it is not the case for nonlinear effects like the transition to the mixed state at the first critical magnetic field. The first critical magnetic field is determined by the energy of the magnetic vortex localized near the normal layer (Josephson vortex). Let us consider the Josephson vortex for the case when the London penetration depth λ is much longer than the thickness L . So two inequalities are satisfied: $\lambda \gg L \gg \zeta_0$. The axis of the straight vortex is in the middle of the normal layer, and at distance r from the axis exceeding L the structure of the vortex does not differ essentially from the Abrikosov vortex in the superconductor bulk. The area $r > L$ gives the logarithmic contribution to the vortex energy per vortex length:

$$E_v = \left(\frac{\Phi_0}{4\pi\lambda}\right)^2 \ln \frac{\lambda}{L}, \quad (69)$$

where $\Phi_0 = hc/2e$ is the magnetic flux quantum. The area $r < L$ adds a number of order unity to the large logarithm. The energy E_v is lower than the energy of the Abrikosov vortex with the coherence length ζ_0 replacing L as a lower cut-off of the logarithm [16]. If $L \gg \lambda$ the vortex energy is even smaller since the large logarithm in Eq. (69) is replaced by a number of order unity. This means that Josephson vortices are pinned to the normal layer, where their energy is less than the energy of Abrikosov vortices in the superconducting layers. The vortex energy determines the first critical magnetic field: $H_{c1} = 4\pi E_v/\Phi_0$.

IX. SUMMARY AND DISCUSSION

Previous investigations of the ballistic SNS sandwich were revised on the basis of our approach, which properly satisfies the charge conservation law and takes into account the incommensurability of the superconducting gap with the Andreev level energy spacing. Let us summarize the main conclusions of this work:

- Due to the effect of incommensurability, in the ground state of a 1D ballistic SNS sandwich the phase difference θ across the sandwich is not necessarily 0, but can take any value between 0 and π . Such a sandwich can be called θ junction. The well known π junction is a particular case $\theta = \pi$ of θ junctions.

- In 1D systems there is no essential suppression of the supercurrent through the ballistic SNS junction at temperatures on the order or higher than the energy distance between Andreev levels, but lower than the superconducting gap.
- Although the ballistic SNS junction has some properties of the Josephson junction, it is not always a weak link in a strict sense. At zero temperature, or temperatures much lower than the Andreev level energy spacing, the weak magnetic field penetrates into the normal layer on the same London penetration depth as into the superconducting layers. There is no Josephson plasma mode localized at the normal layer in this case.
- The structure of magnetic vortices in the ballistic SNS junction essentially differs from structure of usual Josephson vortices, but still have energy lower than the energy of the Abrikosov vortex in the bulk of the superconductor. Therefore, vortices are pinned to the normal layer, and the first critical magnetic field for them is lower than for the superconductor bulk.

Through the whole paper the ballistic SNS sandwich was considered as a Josephson junction. However, it is also possible to describe it not in terms of the Josephson physics. The ballistic normal layer does not destroy the phase coherence and supports the supercurrent $J_s = en_0 v_s$ with the same superfluid velocity v_s and the same density n_0 as in the superconducting layers. The supercurrent is restricted by the Landau criterion that the velocity v_s does not exceeds the Landau critical velocity equal at zero temperature to

$$v_L = \frac{\varepsilon_0}{\hbar k_f} = \frac{\pi \hbar}{2mL}. \quad (70)$$

At this velocity the energy of a quasiparticle at the lowest Andreev level becomes negative due to the Doppler shift. This yields the critical current $J_c = J_0$ given by Eq. (38). Since the Landau critical velocity inversely proportional to the layer thickness L , in the macroscopic (thermodynamic) limit $L \rightarrow \infty$ the Landau critical velocity vanishes. Thus, “superconductivity” of the normal layer in the SNS sandwich is not a macroscopic, but a mesoscopic quantum phenomenon. It is similar to mesoscopic persistent currents in 1D normal metal rings predicted theoretically [23, 24] and observed experimentally (see Ref. 25 and references therein). The values of these persistent currents are of the same order ev_f/L as supercurrents in the ballistic SNS sandwich (for currents in normal rings

L is the circumference length of a ring). The origin of persistent currents was connected with discreteness of energy levels in mesoscopic rings, but incommensurability is also an inevitable consequence of spectrum discreteness. In the case of normal rings this is incommensurability of the Fermi energy (chemical potential) [24], when the number of electrons changes from even to odd value. In the case of SNS sandwiches the number of Andreev levels changes from even to odd.

Analogy with persistent currents in mesoscopic normal ring points out a possible method of experimental investigation of supercurrents in ballistic SNS sandwiches. In normal rings they measured a magnetic moment induced by persistent currents as a function of the magnetic flux threading the ring. One can put the SNS sandwich into a closed electrical circuit loop and make similar measurements. In fact, this idea has already been realized in the experiment on a carbon nanotube junction [9]. A carbon nanotube is a 1D, or, more accurately, nearly a 1D object (small number of active channels). Delagrè *et al.* [9] observed the transition from 0 to π junction in qualitative agreement with our prediction for 1D SNS junctions. Moreover, in the course of this transition they observed a current–phase relation with the period π [see Fig. 4(b)(4) in their paper] two times smaller than the usual period 2π . This is also expected from our analysis [see the paragraph after Eq. (62)].

Delagrè *et al.* [9] interpreted their experiment differently. They considered a nanotube as a quantum dot and connected the $0-\pi$ transition with the Kondo effect. Treating a nanotube as a quantum dot means that the nanotube is rather short and the number of Andreev levels in it is not large. Our analysis is valid in the opposite limit of very long nanotube with large number of Andreev levels. The fact that the $0-\pi$ transition is also predicted in this limit means that the phenomenon is robust and not necessarily connected with the properties of quantum dots and the Kondo effect.

ACKNOWLEDGMENTS

This work was started during my visit to the Low Temperature Laboratory of the Aalto University (Finland) in October 2019. I thank Dmitry Golubev and Pertti Hakonen for numerous discussions and comments, which stimulated my interest to this problem and helped its solution. I am also thankful to the anonymous referee who detected a wrong sign of the vacuum current in the original version of this paper. This led to revision of some its conclusions.

[1] I. O. Kulik, Macroscopic quantization and the proximity effect in SNS junctions, *Zh. Eksp. Teor. Fiz.* **57**, 1745 (1969), [*Sov. Phys.-JETP*, **30**, 944 (1970)].

[2] C. Ishii, Josephson currents through junctions with normal metal barriers, *Prog. Theor. Phys.* **44**, 1525 (1970).
 [3] J. Bardeen and J. L. Johnson, Josephson current flow

- in pure Superconducting-Normal-Superconducting junctions, *Phys. Rev B* **5**, 72 (1972).
- [4] D. Giuliano and I. Affleck, The Josephson current through a long quantum wire, *J. Stat. Mech-Theory E*, P02034 (2013).
 - [5] X.-Z. Yan and C. S. Ting, Supercurrent transferring through *c*-axis cuprate Josephson junctions with thick normal-metal bridge, *J. Phys.: Condens. Matter* **21**, 035701 (2009).
 - [6] V. E. Calado, S. Goswami, G. Nanda, M. Diez, A. R. Akhmerov, K. Watanabe, T. Taniguchi, T. M. Klapwijk, and L. M. K. Vandersypen, Ballistic Josephson junctions in edge-contacted graphene, *Nat. Nanotechnol.* **10**, 761 (2015).
 - [7] M. Zhu, M. Ben Shalom, A. Mishchenko, V. Fal'ko, K. Novoselov, and A. Geim, Supercurrent and multiple Andreev reflections in micrometer-long ballistic graphene Josephson junctions, *Nanoscale* **10**, 3020 (2018).
 - [8] S. Backens and A. Shnirman, Current-phase relation in a topological Josephson junction: Andreev bands versus scattering states, *Phys. Rev. B* **103**, 115423 (2021).
 - [9] R. Delagr ange, R. Weil, A. Kasumov, M. Ferrier, H. Bouchiat, and R. Deblock, $0-\pi$ quantum transition in a carbon nanotube Josephson junction: Universal phase dependence and orbital degeneracy, *Phys. Rev. B* **93**, 195437 (2016).
 - [10] V. V. Ryazanov, V. A. Oboznov, A. Y. Rusanov, A. V. Veretennikov, A. A. Golubov, and J. Aarts, Coupling of two superconductors through a ferromagnet: Evidence for a π junction, *Phys. Rev. Lett.* **86**, 2427 (2001).
 - [11] R. R. Schulz, B. Chesca, B. Goetz, C. W. Schneider, A. Schmehl, H. Bielefeldt, H. Hilgenkamp, J. Mannhart, and C. C. Tsuei, Design and realization of an all *d*-wave dc π -superconducting quantum interference device, *Appl. Phys. Lett.* **76** (2000).
 - [12] J. A. van Dam, Y. V. Nazarov, E. P. A. M. Bakkers, S. D. Franceschi, and L. P. Kouwenhoven, Supercurrent reversal in quantum dots, *Nature* **442**, 667 (2006).
 - [13] A. F. Volkov, New phenomena in Josephson SINIS junctions, *Phys. Rev. Lett.* **74**, 4730 (1995).
 - [14] P. G. de Gennes, *Superconductivity of metals and alloys* (Benjamin, 1966).
 - [15] C. Virgilio Nino and R. Kuemmel, Quantum stability and screening in superconducting metallic weak links, *Phys. Rev. B* **29**, 3957 (1984).
 - [16] M. Tinkham, *Introduction to superconductivity*, 2nd ed. (McGraw-Hill, 1996).
 - [17] E. B. Sonin, Transverse force on a vortex and vortex mass: effects of free bulk and vortex-core bound quasiparticles, *Phys. Rev B* **87**, 134515 (2013).
 - [18] E. B. Sonin, *Dynamics of quantised vortices in superfluids* (Cambridge University Press, 2016).
 - [19] Y. Makhlin and G. E. Volovik, Spectral flow in Josephson junctions and effective Magnus force, *Pis'ma Zh. Eksp. Teor. Fiz.* **62**, 923 (1995), [*JETP Lett.* **62**, 941–946 (1995)].
 - [20] M. Stone, Spectral flow, Magnus force, and mutual friction via the geometric optics limit of Andreev reflection, *Phys. Rev. B* **54**, 13222 (1996).
 - [21] I. S. Gradshteyn and I. M. Ryzhik, *Table of integrals, series, and products*, seventh ed. (Academic Press, 2007).
 - [22] J. M. Luttinger, Fermi surface and some simple equilibrium properties of a system of interacting fermions, *Phys. Rev.* **119**, 1153 (1960).
 - [23] M. B uttiker, Y. Imry, and R. Landauer, Josephson behavior in small normal one-dimensional rings, *Physics Letters A* **96**, 365 (1983).
 - [24] H.-F. Cheung, Y. Gefen, E. K. Riedel, and W.-H. Shih, Persistent currents in small one-dimensional metal rings, *Phys. Rev. B* **37**, 6050 (1988).
 - [25] H. Bluhm, N. C. Koshnick, J. A. Bert, M. E. Huber, and K. A. Moler, Persistent currents in normal metal rings, *Phys. Rev. Lett.* **102**, 136802 (2009).